Int J Mater Form (2014) 7:189–196
DOI 10.1007/s12289-012-1119-2

ORIGINAL RESEARCH

Characterization of rapid PDMS casting technique utilizing molding forms fabricated by 3D rapid prototyping technology (RPT)

Attila Bonyár · Hunor Sántha · Máté Varga · Balázs Ring · András Vitéz · Gábor Harsányi

Received: 6 February 2012 / Accepted: 5 November 2012 / Published online: 11 November 2012

Abstract In this work we characterize a novel possibility for PDMS (PolyDiMethylSiloxane) casting/ micromolding methods with the utilization of molding forms fabricated by a commercially available novel acrylic photopolymer based 3D printing method. The quality and absolute spatial accuracy of 1) different 3D printing modes ('matt' vs. 'glossy'); 2) the molded PDMS structures and 3) the subsequently produced complementary structures made of epoxy resin were investigated. The outcome of these two form transfer technologies were evaluated by the cross sectional analysis of open microfluidic channels (trenches) with various design. Our results reveal the spatial accuracy in terms of real vs. CAD (Computer Aided Design) values for the 3D printed acrylic structures and the limits of their form transfer to PDMS, then to epoxy structures. Additionally the significant differences between the various spatial directions (X, Y, Z) have been characterized, and the conclusion was drawn that the 'glossy' printing mode is not appropriate for 3D printing of microfluidic molds.

Keywords 3D printing · RPT · Microfluidics · PDMS

Introduction

3D RPT (Rapid Prototyping Technology) printing—more specifically photopolymer printing based on Inkjet technology—is a dynamically developing technique used in any industry where prototype parts and physical models are required including aerospace and defense, medical devices, high technology, and manufactory. Current 3D printers tend to achieve such a fine resolution (e.g. 16 μm layer thickness) that makes them utilizable for many microfluidic applications as well. However, the capabilities of 3D printing are not yet fully developed in the field of applied research/ experimental development works, where flexibility and speed are key demands. Based on our literature review, researchers apply 3D printed structural elements only in few cases in experimental science nowadays, for example to realize and supplement fluidic connections [1–3] or in the field of medical diagnosis and treatment e.g. oral surgery [4–6] or cardiology [7]. Novel works present a large variety of advanced technologies applied for microfluidic device fabrication, such as contact liquid photolithographic polymerization [8] or print-and-peel microfabrication [9]. Another recent work introduces a maskless direct writing technique [10] for microfluidic fabrication and also gives an extensive overview about other different rapid prototyping methods for microfluidic devices —except 3D printing. In 2002 McDonald et.al investigated the possibility of utilizing solid-objet printing for microfluidic device fabrication [11], however the feature size of such devices were above 250 μm which is far from the currently available 3D printing resolution (e.g. 42 μm, 82 μm and 16 μm in the X, Y and Z axis respectively).

In one of our previous works the possible utilization of high resolution 3D printing in three different application areas was reported [12], such as the polymer-based microfluidic fabrication method using relatively low-cost 3D RPT molds. The reported total fabrication time of such devices is approx. 3–5 h including the mold printing and polymer casting. PDMS (PolyDiMethylSiloxane) is a versatile material frequently used for various microfluidic purposes due to its excellent molding and optical qualities. It is a great

A. Bonyár (✉) · H. Sántha · M. Varga · B. Ring · A. Vitéz · G. Harsányi
Department of Electronics Technology,
Budapest University of Technology and Economics,
Goldmann square 3,
Budapest 1111, Hungary
e-mail: bonyar@ett.bme.hu

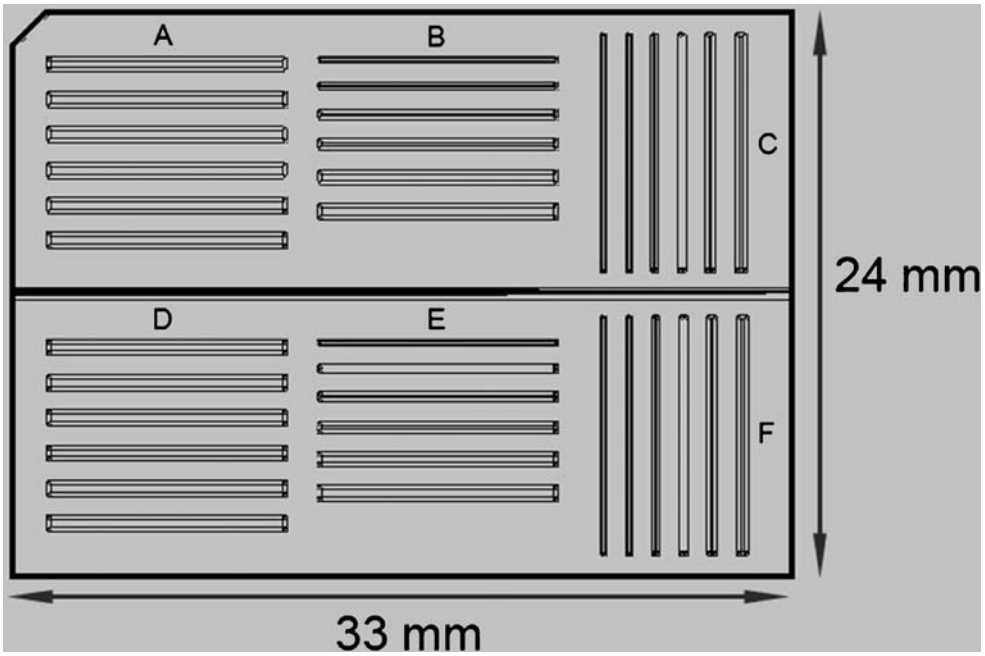

Fig. 1 CAD drawing of the test pieces with 3 columns for investigating 'X', 'Y' and 'Z' directions and 2 rows for investigating the integer and non-integer multiple of the resolution unit

advantage that PDMS microfluidic parts can be bonded irreversibly to glass [13] or to other PDMS parts by means of plasma or corona discharge treatment [14] or double sided adhesive polymer tapes [15]. The most widespread method to fabricate PDMS microfluidic elements is micromolding by the utilization of various molds, such as PMMA (polymethyl methacrylate) [16] or SU-8 structural photoresist [17].

In this work we investigate the limits of application of 1) 3D RPT printed molding forms and 2) epoxy molding forms subsequently produced by deploying the 3D RPT printed molding forms as a master and an intermittent PDMS casting step for the fabrication of PDMS microfluidic structures (e.g. trenches). Besides the above mentioned two types of structures we characterize the PDMS structures themselves too vs. the theoretical values of the CAD design. The spatial resolution and quality of the molding form plays an important role in the process. That is why our primary aim is to characterize 1) the quality and accuracy of the 3D printing in the case of different printing setups ('matt', 'glossy') and 2) the quality of the form transfer techniques to PDMS and epoxy. The epoxy form transfer step is considered as a possible way to fabricate and reproduce more rigid and stable molding forms for PDMS structures, since the acrylic photopolymer-based 3D RPT printed parts and molding forms are very sensitive to temperatures above 45 °C and do not allow quick curing of PDMS at elevated temperatures.

Table 1 Parameters of trenches in the measurement series

Running parameter	z [μm]	y [μm]	x [μm]
Integer multiple of the resolution unit (zones A-C)	16	84	42
	32	168	84
	64	252	126
	96	336	168
	128	420	252
	160	504	336
Non-integer multiple of the resolution unit (zones D-F)	20	80	50
	40	160	100
	80	240	150
	120	320	200
	160	400	250
	200	480	300
Fixed dimension	y=500 μm	z=200 μm	z=200 μm
Length of trench	x=10 mm	x=10 mm	y=10 mm

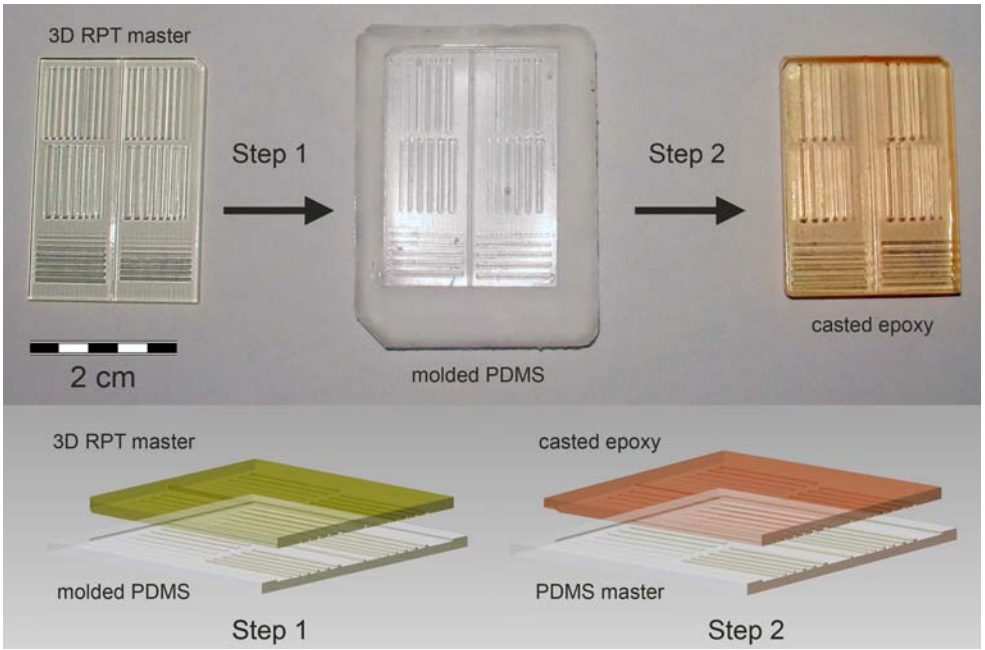

Fig. 2 Illustration of the form transfer technology steps. From left to right: 3D RPT printed molding form, PDMS negative, epoxy positive (can be used as molding form instead of the 3D RPT printed one)

Materials and methods

Materials

Raw PDMS components (Sylgard 184) were purchased from Dow Corning Corp. (USA). FullCure 720 model material and FullCure 705 support material were purchased from Varinex Inc. (Hungary). Raw epoxy components (Eporezit T-111, Epovill A) were purchased from P+M Polymer Chemistry Inc. (Hungary).

3D Printing

For 3D RPT printing an Objet Geometries Eden 250 printer with FullCure 720 model material and FullCure 705 support material was used. The resolution of the printer is 600 dpi (42 μm), 300 dpi (82 μm) and 1600 dpi (16 μm) in the X, Y and Z axis respectively according to its datasheet. All fabricated structures were immersed in 7 % NaOH solution for 30 min after printing to remove all the remaining support material. Autodesk Inventor 2010 software was used for designing the objects.

PDMS casting

Raw PDMS was prepared by adding Sylgard 184 curing agent to Sylgard 184 silicone elastomer in 1:10 m/m ratio. The freshly prepared pure PDMS prepolymer was casted against the 3D RPT fabricated master either in a homemade casting workstation consisting of a vacuum exsiccator, a water stream based vacuum pump and tubing or in a homemade vacuum chamber with a rotary vacuum pump. After removing the bubbles for 10 min in vacuum (pressure below 5 kPa) PDMS was cured at 140 °C for 60 min.

Epoxy casting

Raw epoxy was prepared by adding Eporezit T-111 curing agent to Epovill A epoxy elastomer in 1000:735 m/m ratio. To avoid formation of air bubbles in the final structures the fresh epoxy samples were put into a pressure chamber with

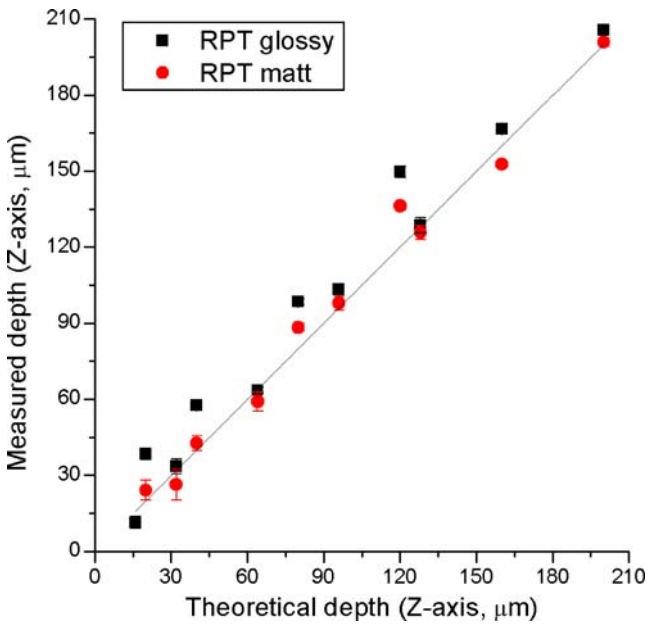

Fig. 3 Theoretical vs. measured channel depths (Z-axis). Squares: 'glossy' printing mode, round: 'matt' printing mode; line: optimal accuracy (measured=theoretical)

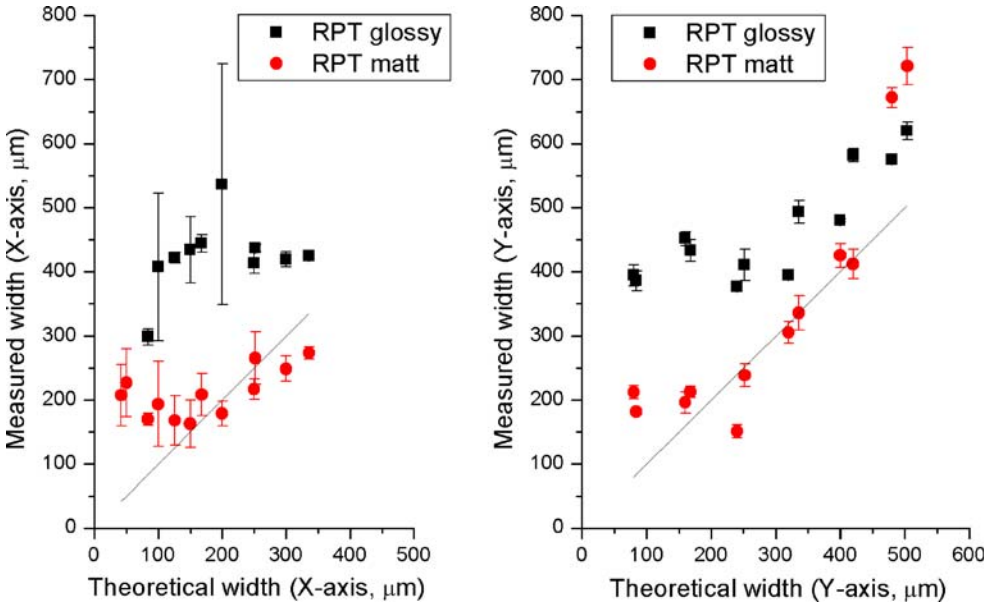

Fig. 4 Theoretical vs. measured channel widths in the X-direction (*left*) and in the Y-direction (*right*). Squares: 'glossy' printing mode, round: 'matt' printing mode; line: optimal accuracy (measured=theoretical)

400 kPa overpressure for 25 min. Afterwards the molded epoxy parts were heated to 120 °C for 40 min in order for hardening.

Measurement series

Test pieces were designed with 6 structural zones (A–F) according to the schematics presented in Fig. 1.

Table 1 collects the parameters of trenches designed for the measurement series testing the spatial accuracy of the 3D printing and the two form transfer technologies. The measurement series is designed in a way that enables the test of the spatial resolution of the printer in integer multiples of its theoretical resolution units, (which is 42 μm, 82 μm and 16 μm in the X, Y and Z axis, respectively) and also in non-integer multiples of the resolution. The length of each trench was 10 mm; the distance between the trenches was 1 mm.

Figure 2 illustrates the steps of the form transfer technology process.

Profile measurements

The profiles of trenches were measured with an Alpha Step 500 surface profiler from Tencor Instruments. The length of the profiler needle was 880 μm with a tip angle of 60°. The applied scanning speed was 0.1 mm/s with a resolution of 2 μm. The exported profiles were evaluated with custom Matlab software obtaining and evaluating 5 cross section profiles from each section taken at ca. 1, 3, 5, 7 and 9 mm

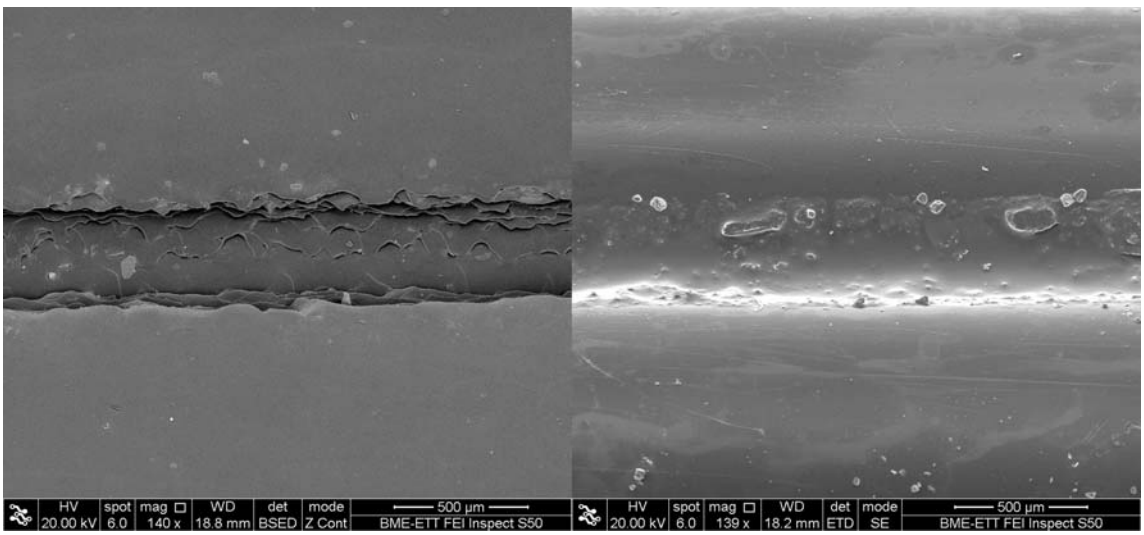

Fig. 5 Scanning Electron Microscope (SEM) images of the channels printed in 'matt' (*left*) and 'glossy' (*right*) mode

along the axis of the 10 mm long trenches. The channel width was measured at 50 % depth levels of the trenches.

Results and discussion

Validation of the spatial accuracy of printing

As the first step, the spatial accuracy of the Objet Eden 250 printer was measured and compared for the two printing modes ('matt', 'glossy'). Our results shown in Fig. 3 indicate that the measured depths values are close to the theoretical values from the CAD plan (straight line) and reveal that 'matt' printing mode provides higher accuracy. The average deviation from the theoretical depth values is 12.8 % for the 'matt' mode and 21.2 % for the 'glossy' mode calculated for the whole measurement range (from 16 μm to 200 μm). Since the printer works with 16 μm thick layers in the Z direction, the designed depths values which are non-integer multiples of this value are realized with an extra 16 μm thick layer. Hence, as it can be seen in Fig. 3, the printer is more accurate when the designed channel depth is integer multiple of the resolution. The average deviation from the theoretical depth values is 7.3 % for the 'matt' mode and 9.9 % for the 'glossy' mode calculated for the channel depths, which are an integer multiple of the resolution.

Figure 4 compares the theoretical and measured width values of trenches in the Y and X directions, respectively. The accuracy of the 'glossy' printing mode is unacceptably low, the average deviation between the theoretical and printed width of the channels is 115.2 % in the X and 152.4 % in the Y direction for the whole measurement range (but only 33.5 % and 51.2 % in the X and Y dimensions respectively for channels above 250 μm widths). In comparison, for the 'matt' mode the same average deviation is 39.2 % and 89.7 % in the X and Y directions respectively for the whole range (and only 18.7 % and 13.9 % for channels above 150 μm widths). The widening of the channels printed in 'glossy' mode is probably due to the lack of support material used for the printing in 'matt' mode, which causes the channel walls to deform after the deposition of the acrylic model layer. The 'glossy' printing mode is applied in such cases when the transparency of the printed part and outer surfaces with less light-scattering are important. This mode enables the surface roughness of these samples to be somewhat better than the samples printed in 'matt' mode (an average R_a of 0.59 μm compared to 0.78 μm according to the cumulated analysis of our whole measurement series). This means, that it is easier to remove the PDMS from the 'glossy' masters than from the masters printed in 'matt' mode which could be important in the case of structures that have high depth/width ratio.

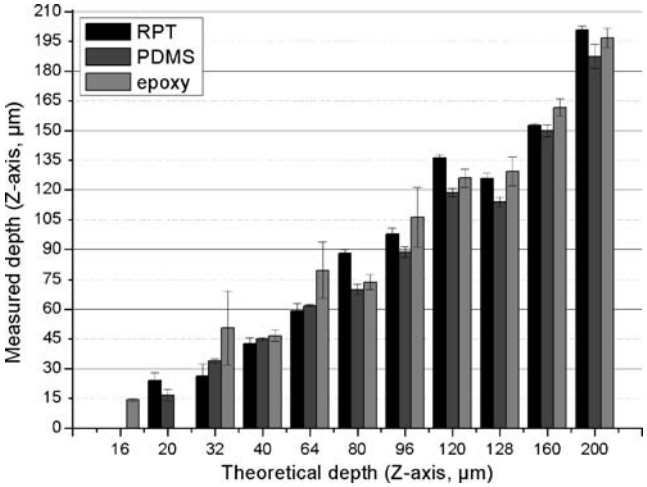

Fig. 6 Theoretical vs. measured depth values in the subsequent phases of the form transfer technology in 'matt' mode. (Note: the following data are missing from the graph: RPT-16 μm, PDMS-16 μm, epoxy-20 μm)

Figure 5 presents sample scanning electron microscope (SEM) images of the two different printing modes. It can be seen that the 'glossy' printing mode results in much smoother features. However, if these aspects are less important, the 'glossy' mode is not advised for microfluidic applications below the 400 μm range due to its low printing accuracy based on these results. We have to mention that the correction of the channel distortion in the X and Y dimensions could be possible by changing the CAD design, but since the change of the features are structure dependent the user has to characterize and design the compensation for every custom structure in 'glossy' mode.

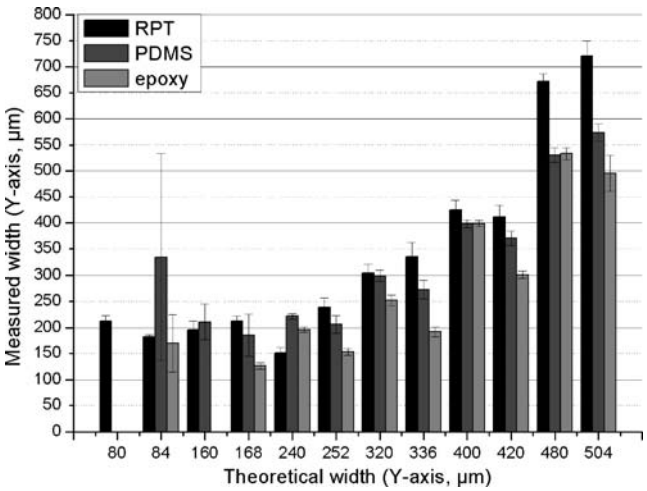

Fig. 7 Theoretical vs. measured Y-dimensional width values in the subsequent phases of the form transfer technology in 'matt' mode. (Note: the following data are missing from the graph: PDMS-80 μm, epoxy-80, 160 μm)

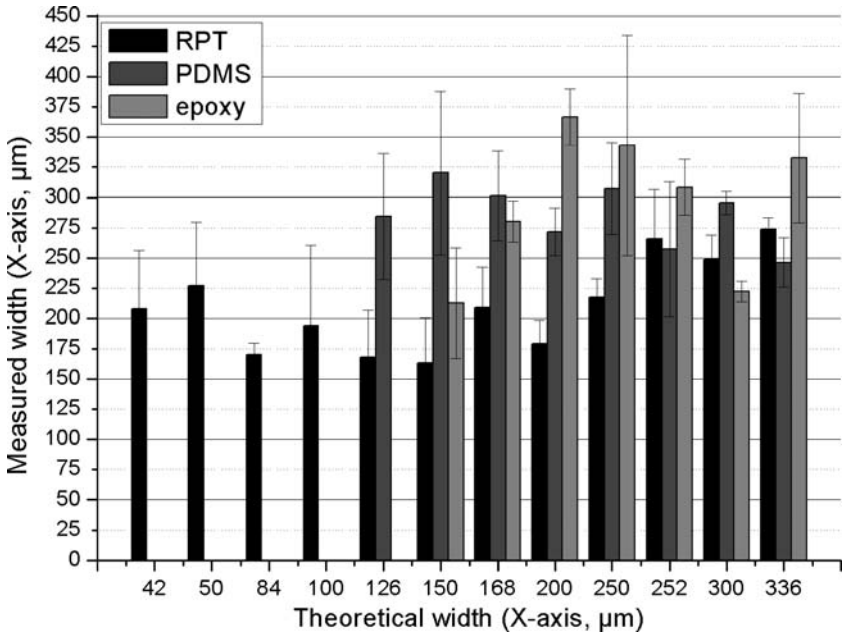

Fig. 8 Theoretical vs. measured X-dimensional width values in the subsequent phases of the form transfer technology in 'matt' mode. (Note: the following data are missing from the graph: PDMS-42, 50, 84, 100 μm, epoxy-42, 50, 84, 100, 126 μm)

The leaning and widening of the trench walls also occur in 'matt' mode, especially for dimensions below 200 μm for the Y-direction and below 150 μm for the X-direction. The Y direction of the printer seems to be more accurate, despite the fact that it is the one which, according to the user manual of the 3D printer has lower resolution. Considering this contradiction the authors maintain the possibility that the printing directions are mixed up in the supplied software of the Objet Eden 250 printer used.

Based on these results we only validated the accuracy of the form transfer technologies that utilize masters printed in 'matt' mode, as it can be seen in the next chapter.

Accuracy of the form transfer technology

Figures 6, 7 and 8 compare the theoretical (i.e. in the CAD plan) and measured dimensions of the trenches in the different steps of the polymer casting based form transfer. It can be seen, that the depth values are transferred with acceptable accuracy (94.65 % +/−16 % for the PDMS transfer and 115.57 % +/−15 % for the epoxy transfer, calculated fort the whole measurement range).

Considering the planar resolution, above 160 μm in the Y-dimension the width values decrease after the PDMS and subsequent epoxy casting. In the X-dimension the results are

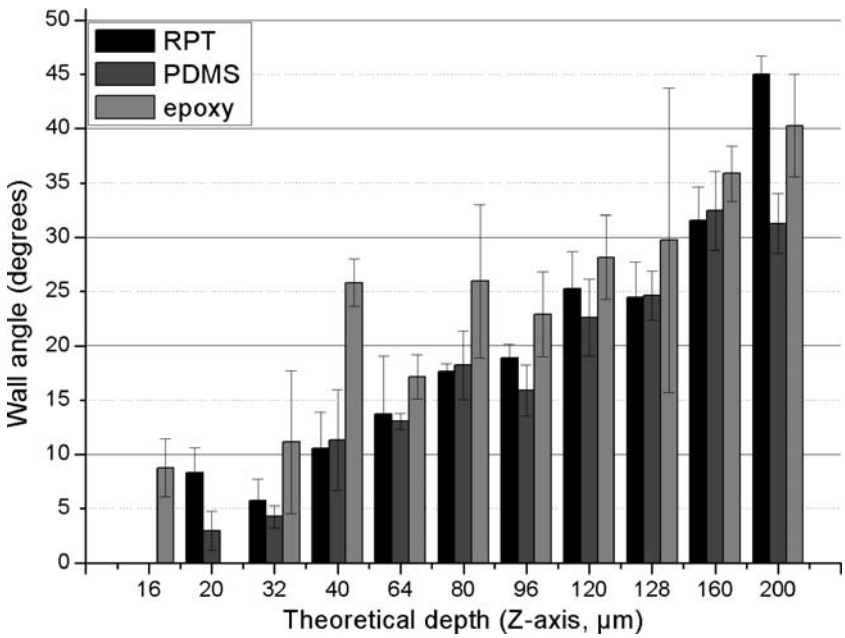

Fig. 9 Theoretical channel depth vs. measured channel angle in the subsequent phases of the transfer technology in 'matt' mode. (Note: the following data are missing from the graph: RPT-16 μm, PDMS-16 μm, epoxy-20 μm)

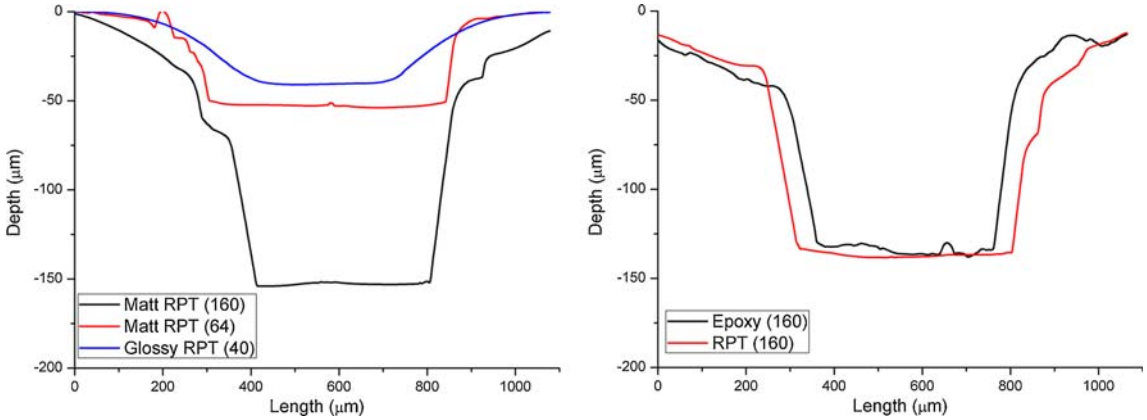

Fig. 10 Channel wall profiles for the illustration of the wall angle for various channel depths. *Left*: 'matt' RPT Channel (theoretical depth 160 μm), 'matt' RPT channel (64 μm), 'glossy' RPT channel (40 μm); *right*: 'matt' RPT channel (160 μm) and the same channel after epoxy molding. For all the channels the theoretical width is 150 μm

the opposite: the width values increase similarly to the standard deviations. We can conclude that according to these results the form transfer in the Y-dimension is more accurate and thus this direction should be selected as width for printing of trenches.

Figure 9 shows the measured wall angle of the trenches in the function of the depth values. The wall angles are very low which also confirms that the walls lean after the polymer deposition during printing, even in the case of 'matt' printing. As a consequence the trenches widen and thus the width of a trench is limited in the X and Y dimensions to 200 μm for 'matt' mode and to 400 μm for 'glossy' mode, as can be seen in Figs. 3 and 4. The results also indicate that the angle of the walls increases significantly with the depth values. Apart from this it increases after the epoxy molding. This is a positive side effect which means that the epoxy resin somehow compensates the flaws in the PDMS channel. Figure 10 left illustrates the angle difference between channels printed in matt and glossy mode in various depths, while Fig. 10 right shows the effect of the epoxy molding on the wall angle.

The surface roughness of the structures increased significantly in each step of the transfer technology (R_a=0.78 μm; 1.52 μm; 1.96 μm for the RPT, PDMS and epoxy steps respectively, the calculation was performed for cumulated data obtained from all the measurements done).

Considering our findings and the operating principle of the Objet Polyjet technology, which always runs a rolling cylinder over the last printed acrylic layer before the UV illumination step, our hypothesis is the following: by avoiding the slim structures parallel to the X-direction, namely diagonally oriented trenches and arcs in the design, it is possible to approach the planar accuracy found along the Y-axis. In the near future our work will be focused on the validation of this hypothesis.

Conclusions

The printing accuracy of the two printing modes ('matt', 'glossy') of the Objet Eden 250 3D RPT printer was compared along with the accuracy of PDMS and epoxy transfer technologies. We found, that although the 'glossy' printing mode yields fully transparent parts with smaller surface roughness, only the parts printed in 'matt' mode could be applied for microfluidic purposes with acceptable accuracy in the Y, and X directions. The low angle of the walls, which was caused by the leaning of the photopolymer material after deposition induces channel widening, which limits the achievable minimal channel width to 200 μm for 'matt' mode and 400 μm for 'glossy' mode. The Z directional accuracy of the printing is adequate for both modes, but it was also found to be better in the case of 'matt' printing. The PDMS and epoxy transfers yielded successful geometry transition in the Z direction, however in the Y direction a decrease while in the X direction a significant increase was observed in the transferred channel width. Based on the results the Y-direction of the printer is suggested to be used for more accurate channel widths. We also found that the angle of the channels increases after the epoxy molding, and that the surface roughness (R_a) of the structures increases in both polymer transfer steps.

Acknowledgments The authors would like to thank for the financial support of the following EC funded FP6 projects: DVT-IMP (FP6-2005-IST-5- 034256), DINAMICS (IP 026804-2), RASP (SP5A-CT-2006-044515); Hungarian Jedlik Ányos Programme: SPE_SAFE (Contract nr. NKFP_07-A2-2008-0268). This work is connected to the scientific program of the " Development of quality-oriented and harmonized R+D+I strategy and functional model at BME" project. This project is supported by the New Hungary Development Plan (Project ID: TÁMOP-4.2.1/B-09/1/KMR-2010-0002).

References

1. Lee D, Sukumar P, Mahyuddin A, Choolani M, Xua G (2010) Separation of model mixtures of epsilon-globin positive fetal nucleated red blood cells and anucleate erythrocytes using a microfluidic device. J Chromatogr A 1217:1862–1866
2. Hu M, Deng R, Schumacher KM, Kurisawa M, Ye H, Purnamawati K, Ying JY (2010) Hydrodynamic spinning of hydrogel fibers. Biomaterials 31:863–869
3. Piliarik M, Vala M, Tichy I, Homola J (2009) Compact and low-cost biosensor based on novel approach to spectroscopy of surface plasmons. Biosens Bioelectron 24:3430–3435
4. Faber J, Berto PM, Quaresma M (2006) Rapid prototyping as a tool for diagnosis and treatment planning for maxillary canine impaction. Am J Orthod Dentofacial Orthop 129(4):583–589
5. Ciuffolo F, Epifania E, Duranti G, De Luca V, Raviglia D, Rezza S, Festa F (2006) Rapid prototyping: a new method of preparing trays for indirect bonding. Am J Orthod Dentofacial Orthop 129(4):75–77
6. Cohen A, Laviv A, Berman P, Nashef R, Abu-Tair J (2009) Mandibular reconstruction using stereolithographic 3-dimensional printing modeling technology. Oral Surg Oral Med Oral Pathol Oral Radiol Endod 108(5):661–666
7. Kim MS, Hansgen AR, Carroll JD (2008) Use of rapid prototyping in the care of patients with structural heart disease. Trends Cardiovasc Med 18(6):210–216
8. Haraldsson KT, Hutchison JB, Sebra RP, Good BT, Anseth KS, Bowman CN (2006) 3D polymeric microfluidic device fabrication via contact liquid photolithographic polymerization (CLiPP). Sensor Actuator B 113:454–460
9. Thomas MS, Millare B, Clift JM, Bao D, Hong C, Vullev VI (2009) Print-and-peel fabrication for microfluidics: what's in it for biomedical applications? Ann Biomed Eng 38 (1):21–32
10. Do J, Zhang JY, Klapperich CM (2011) Maskless writing of microfluidics: Rapid prototyping of 3D microfluidics using scratch on a polymer substrate. Robot Comput Integr Manuf 27(2):245–248
11. Cooper McDonald J, Chabinyc ML, Metallo SJ, Anderson JR, Stroock AD, Whitesides GM (2002) Prototyping of microfluidic devices in poly(dimethylsiloxane) using solid-object printing. Anal Chem 74:1537–1545
12. Bonyár A, Sántha H, Ring B, Varga M, Kovács JG, Harsányi G (2010) 3D Rapid prototyping technology (RPT) as a powerful tool in microfluidic development. Procedia Engineering 5:291–294
13. Plecis A, Chen Y (2008) Improved glass–PDMS–glass device technology for accurate measurements of electro-osmotic mobilities. Microelectron Eng 85:1334–1336
14. Haubert K, Drier T, Beebe D (2006) PDMS bonding by means of a portable, low-cost corona system. Lab Chip 6:1548–1549
15. Kim J, Surapaneni R, Gale BK (2009) Rapid prototyping of microfluidic systems using a PDMS/polymer tape composite. Lab Chip 9:1290–1293
16. Shih T-K, Chen C-F, Ho J-R, Chuang F-T (2006) Fabrication of PDMS (polydimethylsiloxane) microlens and diffuser using replica molding. Microelectron Eng 83:2499–2503
17. Berdichevsky Y, Khandurina J, Guttman A, Lo Y-H (2004) UV/ozone modification of poly(dimethylsiloxane) microfluidic channels. Sensor Actuator B 97:402–408